CALIBRATION OF PORTABLE HPGe SPECTROMETER FOR INDOOR DOSE RATE ESTIMATIONS

A. Clouvas, M. Antonopoulos-Domis and S. Xanthos

Department of Electrical and Computer Engineering,
Aristotle University of Thessaloniki,
GR.-54006 Thessaloniki

INTRODUCTION

In situ gamma spectrometry is a powerful tool to study indoor and outdoor dose rates. A high resolution spectrum allowing analysis of individual photo peaks provides valuable information on the relative contribution of the various nuclides to the total exposure rates. In situ techniques for measuring the dose rate, resulting from the gamma radiation and characterizing its sources, with a gamma ray spectrometer have been used successfully in the outdoor environment (1-4). In principle, the same methods can be applied to indoor radiation measurements. However, due to complex or generally unknown geometry in indoor areas, the methods for outdoor environments can not be applied directly to indoor ones. In the present work we investigate the applicability of the calibration factors derived from field geometry to indoor geometry.

METHODOLOGY

In order to check whether calibration factors for field geometry can be applied to indoor radiation measurements, we applied to our measured indoor and outdoor spectra a geometry independent method, the spectral stripping method (5), (6), for determining the gamma dose rates, which does not require any assumptions concerning the source geometry. The measured indoor and outdoor spectra were performed with a portable coaxial HPGe detector (10% efficiency).

A count registered by the detector can be caused by the full or partial absorption of an incident photon or by the passage of a cosmic ray produced charged particle. In order to convert to gamma dose rate, the spectrum must be stripped of the partial absorption and cosmic-ray events leaving only the events corresponding to the full absorption of a gamma ray. The resulting spectrum, which represents both primary as well as scattered photons, can then be converted to the total incident flux spectrum by applying the full absorption efficiency curve of the detector.

The flux spectrum is then used to calculate the total gamma dose rate which can be compared with the sum of the individual dose rates for each radionuclide (natural and man-made) obtained with the use of the calibration factors for field geometry. When these two values are in agreement, one can assume that the calibration factors being used are correct.

Concerning the cosmic-ray events induced in the detector we followed the methodology given in ref. (5), (6). The cosmic ray count rate in the region below 3 MeV in a typical Ge detector is generally small compared to the gamma count rate. Since there is no natural gamma line present between 3 and 4 MeV, this region is used to estimate the cosmic ray count rate which is then extrapolated back to 0 MeV and subtracted out from the spectrum. Although there may be some variation in the energy distribution, we have assumed as in ref. (5), (6) that the cosmic continuum is flat in this region.

Concerning the partial absorption events induced in the detector we followed the methodology given in ref. (5), (6) and ref. (7).The events corresponding to partial absorption in the detector make up a large fraction of the counts in the spectrum and are not as simple to strip out. For the most part, these events are the result of compton scatter in the crystal itself or the surrounding cryostat. For single scatter events, a continuum of counts will form in the spectrum reaching a maximum energy at the compton edge given by

$$E_c = E_p - \left(\frac{2}{0.511} + \frac{1}{E_p} \right)^{-1} \quad (1)$$

where E_c is the energy of the Compton edge and E_p is the energy of the incident gamma ray.

Okano et al (7) have used a distribution of counts with energy which is essentially a single step function between the low end of the spectra and E_c. An example of the actual distribution of counts in the continuum for normal incident 0.662 MeV photons in our detector is shown in Figure 1. It can be seen that: (a) the energy dependence below Ec can not be described by a constant and (b) there are a number of counts that lie above E_c, which are a result of multiple scatter events within the crystal. Based on this, Miller (5), (6) incorporated into the stripping routine, a multiple step function fit to the continuum. In our method which is simple, quick and acceptable accurate, a two function fit to the continuum was incorporated into the stripping routine. The region below E_c is fitted with a polynomial function of second order and the region between E_c and E_p with the sum of an exponential and linear function. The different parameters of the polynomial and exponential function depend on the incident photon energy and have been obtained assuming a constant Peak to Compton ratio for all energies. For incident photons 0.662 MeV, the polynomial and exponential functions used in the stripping routine are also shown in Figure 1. The correlation coefficients between measured and fitted data for the fist region, (100 keV until E_c) and the second one (E_c until E_p) are 0.76 and 0.99 respectively. It should be noted also, that when we write Peak to Compton ratio, we mean the number of counts at E_p divided by the average number of counts in the channels for the range from $0.99 \cdot E_c$ through E_c, and not the one given by the manufacturer, which is determined as the ratio which is found by dividing the number of counts in the 1.332 MeV peak channel by the average number of counts in the channels for the range from 1.040 through 1.096 MeV. One must have in mind that the number of counts in the peak

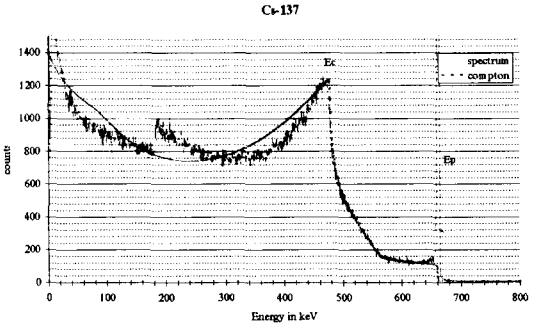

Figure 1. Cs-137 spectrum and compton fit.

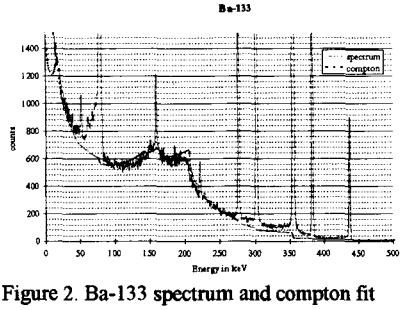

Figure 2. Ba-133 spectrum and compton fit

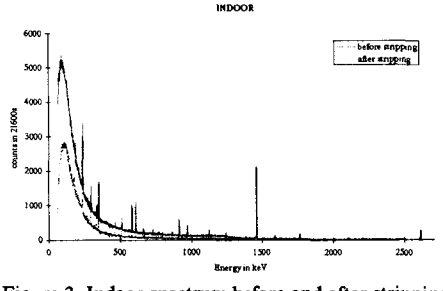

Figure 3. Indoor spectrum before and after stripping

(E_p) are considerably higher that the counts in the Compton edge (E_c).

Using the assumed shapes for the cosmic and partial absorption continua we proceed to a computerized stripping operation which subtracts out from the measured in-situ spectrum those counts that represent cosmic-ray events or partial absorption of gamma rays in the detector. The stripping operation is initiated at the highest energy gamma peak (2.615 MeV) and involves subtracting the assumed continuum of counts which is lower in energy. The operation continues for succeeding lower energies gamma peaks down to 100 keV. In order to check our stripping operation we test it in a spectrum obtained with incident γ rays emitted from a Co-60 and Ba-133 point sources. It can be seen in Figure 2, that the compton distribution deduced from the stripping operation describes successfully the experimental values.

An example of a stripped indoor spectrum as compared to the original spectrum is shown in Figure. 3. Typically about 50% of the counts are removed. These counts are removed from the continuum portion of the spectrum, while the peaks due to the full absorption of primary flux are preserved. The stripped spectrum of Fig. 3 is converted to incident flux by applying the full absorption efficiency of the detector.

Having calculated the flux energy distribution $\varphi(E)$ the absorbed dose rate in air due to the gamma radiation can be easily calculated by

$$\dot{D} = \int_0^{E_{max}} \varphi(E) \cdot E \cdot \mu(E) \cdot dE \qquad (2)$$

where $\mu(E)$ is the mass absorption coefficient for air at energy E and E_{max} is the highest energy gamma line (2.615 MeV).

RESULTS AND DISCUSSION

In order to check the applicability of the field calibration factors to indoor geometry we performed long duration measurements (six hours). Specifically 5 measurements took place in buildings and 6 in outdoor environments, with 3 of them on roads and pavements. For each spectrum we calculated the total external dose rate (nGy/h) using 3 different methods. (a) The field calibration factors assuming equilibrium along the various nuclides in the U and Th series, so that the measurement of any one spectral line yields concentration values for the entire series, although averaging several spectral lines will give a more precise value. For the U-series we used the lines of 0.352 MeV (Pb-214) and 0.609 MeV (Bi-214) and for the Th-series the lines of 0.583 MeV (Tl-208) and 0.911 MeV (Ac-228). We also measured the lines 1.461 MeV (K-40) and 0.662 MeV (Cs-137). (b) The field calibration factors without assuming equilibrium along the various nuclides in the U and Th series, using equation 2 for the unscattered photons and multiplying the resultant dose rate for each energy with the appropriate build up factor (8). (c) The spectral striping method using equation 2. The results are shown in Table 1.

	using field factors (assuming equilibrium)	**using eq. 2 (without assuming equilibrium)**	**using stripping method**	**field factors to stripping method ratio**
Building	46.7	48.0	53.6	0.87
Building	48.5	49.3	53.23	0.91
Building	49.3	46.3	45.33	1.09
Building	58.4	59.7	63.65	0.92
Building	61.7	62.8	63.98	0.96
Road & Pavement	16.5	15.0	22	0.75
Road & Pavement	31.4	30.7	35.85	0.87
Road & Pavement	32.3	33.5	38.43	0.84
Over Soil	39.0	38.0	36.9	1.06
Over Soil	44.8	44.0	45.13	0.99
Over Soil	44.9	44.2	44.05	1.02

Table 1. Total external dose rate in air (nGy/h)

The fact that the field factors have been verified for the outdoor environment indicate that the stripping operation used is accurate. This can be seen from the ratio between the dose rates estimated by field factors and the stripping operation for measurements over soil, in Table 1.

One can see, observing mainly the results for buildings and houses, that disequilibrium in the U series due to exhalation of Rn-222, from the soil surface or the building materials, does not affect the total dose rate significantly. Also, it is notable, that the use of field calibration factors for roads and pavements underpredict the dose rate

The generally good agreement between the two dose rate estimates between calibration factors and stripping method, which has been observed also for almost all indoor spectra, used for this test, justify the applicability of field geometry factors to indoor geometry at least in the case of masonry structure which is typical for most of the buildings and houses in Greece.

REFERENCES

1. I. HELFER and K. MILLER, Health Phys. 55, 15-29, (1988).
2. N. CUTSHALL and I. LARSEN, Health Phys. 51, 53-59, (1986).
3. C.V. GOGOLAK, IEEE Trans. Nucl. Sci., NS-29-3, 1216-1224, (1982).
4. H.L. BECK, J. De CAMPO, C.V. GOGOLAK, HASL-258, (1972).
5. K.M.MILLER, H.L. BECK, Radiat. Protec. Dosim, 7, 185-189, (1984).
6. K. M. Miller, EML-419, (1984).
7. M. OKANO et al., Natural Radiation Environment III, U.S. Department of Energy Report CONF-780422, Vol. 2 896-911, (1980).
8. H.L. BECK, G. DE PLANQUE, HASL-195, (1968)